PSR internal report

Presented at X SEPOPE Conference, Florianopolis, Brazil, May 2006

Integrated electricity-gas operations planning in long-term hydroscheduling based on stochastic models

B. Bezerra* L.A.Barroso* R.Kelman* B.Flach*

M.L.Latorre* N.Campodonico* M.Pereira*

Abstract: the integration of natural gas and electricity sectors has increased sharply in the last decade as a consequence of combined cycle natural gas thermal power plants. In some countries such as Brazil, gas-fired generation has been a major factor in the overall growth of natural gas consumption. When related to the operations planning, in some hydrothermal systems a National System Operator dispatches these gas-fired plants (along with other thermal sources such as coal, oil and nuclear) in conjunction with the country's hydroelectric plants using a production-costing model based on stochastic programming. The algorithm determines the optimal hydro-to-thermal energy production ratio based on the expected benefit of reducing thermal plant generation over a large number of hydrological scenarios, along a planning horizon of some years. This means that the optimal scheduling decision today depends on assumptions about future load growth and future entrance of new generation capacity. Stochastic dynamic programming models are extensively used. However, the hydrothermal scheduling models usually do not take into account the possibility of future fuel supply constraints, either in production or in transportation. The assumption of fuel supply adequacy is felt to be reasonable for the more mature markets such as coal and oil. However, due to the fast growth of the natural gas market, it is possible that demand outpaces supply and/or transportation investments. Indications that gas-related constraints could be relevant were observed in New England, in the US, and Brazil in 2004, where several MW of combined-cycle generation could not be dispatched when needed due to constraints in pipeline capacity. The objective of this work is present a methodology for representing the natural gas supply, demand and transportation network in the stochastic hydrothermal power scheduling model. The application of the integrated electricity-gas scheduling model is illustrated in case studies with realistic configurations of the 90 GW Brazilian system.

KEYWORDS

Natural gas industry, Hydroelectric-thermal power generation, stochastic dual dynamic programming.

1. Introduction

The integration of natural gas and electricity sectors was intensified in the last decade as consequence of a widespread construction of new gas-fired power plants, both combined-cycle and single-cycle. Several countries in South America, Europe, Asia and the US built a lot of gas-fired generation in order to have a more economical and clean resource than the standard coal and oil-fired resources.

On the operational side, the integration between gas-fired and hydro plants in hydro-based systems is usually not straightforward (due to the low cost of hydro), as opposed to the case of thermal systems.

In some hydro-based systems, specially those in South America (such as Brazil, Chile, Argentina, etc), both hydro and thermal plants are dispatched by the country's National System Operator with basis on a production-costing model. This model determines the optimal hydro-to-thermal energy production ratio based on the expected benefit of reducing thermal plant generation over a large number of hydrological scenarios, along a planning horizon of five year and based on stochastic dynamic programming techniques. This means that the optimal scheduling decision today depends on assumptions about future load growth and future entrance of new generation capacity. However, the hydrothermal scheduling model does not take into account the possibility of future fuel supply constraints, either in production or in transportation. The assumption of fuel supply adequacy is felt to

*Authors affiliation: all authors are with PSR, Rio de Janeiro, Brazil (contact author: luiz@psr-inc.com)

be reasonable for the more mature markets such as coal and oil. However, due to the fast growth of the natural gas market, it is possible that demand outpaces supply and/or transportation investments.

This actually has been observed in some countries. Brazil, for example, built over 7,000 MW of gas-fired generation in the last five years. These gas-fired plants, along with other thermal sources such as coal, oil and nuclear, correspond to 15% of the country's installed capacity; the major source of power production being hydroelectric power. A first indication that gas-related constraints could be relevant took place in January 2004, when 800 MW of combined-cycle generation (out of a total capacity of 1200 MW) could not be dispatched due to constraints in pipeline capacity. In the same vein, the ISO New England commanded the dispatch of about 3000 MW of gas-fired generation in 2004 which turned out to be not available due to lack of natural gas [13].

Coordinating these two sectors, especially for hydro systems is a critical issue. If gas production and transportation constraints are ignored, the scheduler may be optimistic with respect to the firm capacity of the thermal plants, and jeopardize the supply reliability: hydro reservoirs may be depleted faster today based on the availability of future gas-fired generation that may not occur.

The objective of this work is present a methodology for representing the natural gas supply, demand and transportation network in the stochastic hydrothermal power scheduling model used to schedule real hydro-power systems. This will be done in two steps. The first step consists in developing a model to examine the feasibility of the gas-based generation resulting from a hydrothermal scheduling tool from the gas sector side. The objective of the model is to schedule the natural gas supply to meet the total natural gas demand in each node of the gas network, while minimizing the total amount of gas for use by the power sector that is rationed. The second step consists in explicitly introducing the natural gas constraints in the dynamic programming recursion of the energy planning model. Gas demand in each node is given by the sum of non-power gas consumption forecasts plus gas consumption factors for the gas-fired power plants; gas production in each node is represented as minimum and maximum production levels, depending for example if the gas field is associated with oil production. Finally, fuel transportation is modeled both through pipelines and through LNG.

An application illustrating the proposed methodology will be done using the 90 GW Brazilian hydro system as example. The Brazilian system provides good case-studies for the methodology because it has a large-scale hydro system, but, on the other hand, the gas sector is developing at aggressive growth rates and gas-fired plants account for an important share of overall thermoelectric resources. Therefore, it concentrates several characteristics and challenges which are of interest to several other power systems worldwide.

This work is organized as follows: Section 2 presents an overview of the electricity and gas sectors in Brazil. Section 3 describes and motivates the main issues in the energy-gas integration in the country. Section 4 presents a procedure that has been developed for assessing the feasibility of the schedules of the gas-fired power plants. Section 5 presents the integrated representation of the electricity-gas sectors in a hydrothermal scheduling model and Section 6 concludes.

2. Overview of Electricity and Gas Sectors

Brazil is the largest electricity market in South America, accounting for 40% of the continent's energy consumption. As mentioned in the Introduction, the country is hydro-dominated: 85% of the 90 GW installed capacity and more than 90% of the electricity production (44 average GW) comes from hydropower. Thermal generation includes nuclear, coal, diesel, biomass and, more recently, natural gas plants. The country is fully interconnected at the bulk power level by a 80,000 km meshed high-voltage transmission network, shown in Figure 1. The direct international interconnections are the back-to-back links with Argentina (2,200 MW) and smaller interconnections with Uruguay and Venezuela.

On the natural gas side, Brazil has proven gas reserves of 320 bcm [1,2]. The country also has a natural gas production[1] of about 27 MMm^3/day available to the market, mostly associated with the exploration of oil. Since 1999 up to 30 MMm^3/day of imported natural gas has been flowing into the country through pipelines from Bolivia and Argentina. In 2003 a discovery of a large offshore natural gas field (Santos field), capable of more than doubling the country's reserves, was announced.

In contrast with Argentina and Chile, Brazil's gas market is relatively undeveloped. One of the reasons is that there is no market for space heating, which is an important factor in the other countries.

Figure 2 shows the gas pipelines and the areas of exploration and production. There are three separate systems: the largest comprises the South and Southeast regions; coastal cities from the Northeast form the country's second natural gas system; the third system is in the Amazon region.

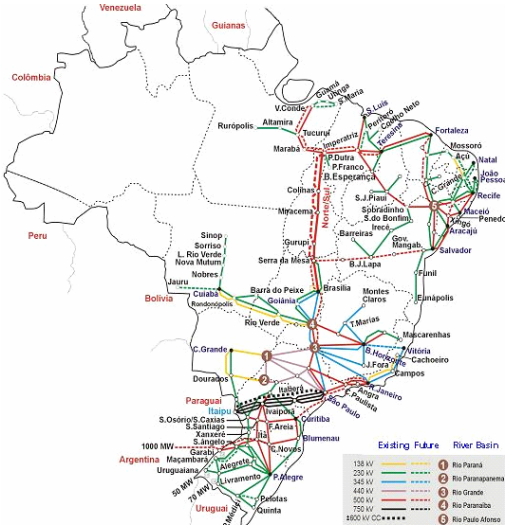

Figure 1 – Power Transmission network, (source ONS)

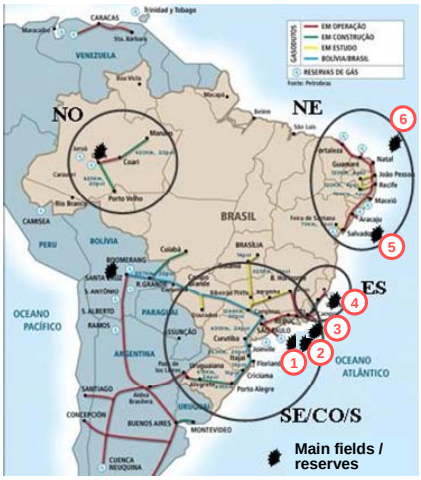

Figure 2 – Natural gas network (source ANP & PSR)

Finally, a Natural Gas law which regulates pipeline access and other topics is currently being discussed in Congress.

3. Electricity-natural gas integration issues

As mentioned previously, Brazil has 7000 MW of gas-fired plants. Their potential gas consumption is quite significant: if dispatched simultaneously, the gas-fired plants would use 35 MMm^3/day of gas, about the same amount as the entire "non-power" gas demand. Also as mentioned previously, the thermal plants' dispatch depends on the hydrological conditions: if the system is "wet", the entire electricity load can be met with hydro generation alone.

In other words, power-related gas consumption is both large and stochastic. This creates a complex problem for investment decisions in new gas fields and in new pipelines, which may be either excessive or insufficient, depending on hydrological conditions. Although take or pay contracts can alleviate part of the financial uncertainty, a mismatch between gas supply and demand can have significant consequences for power scheduling. One example of this mismatch happened in January 2004, when a shortage of hydropower in the Northeast of Brazil made ONS command the dispatch of 1,200 MW of gas-fired plants of the region and only a third of this (400 MW) was delivered due to gas production and transportation constraints. This episode showed the need for greater coordination between the electricity and the natural gas sectors' operations planning. This will be discussed next.

[1] This number excludes reinjection, E&P consumption and flares & losses

4. Probabilistic evaluation of gas-fired plant schedules

We initially developed a probabilistic model for evaluating whether the sum of gas consumption requirements resulting from the hydrothermal dispatch and of "non-power" gas consumption forecasts could be adequately supplied by the existing and planned gas fields and pipeline network. Figure 3 shows the information flow.

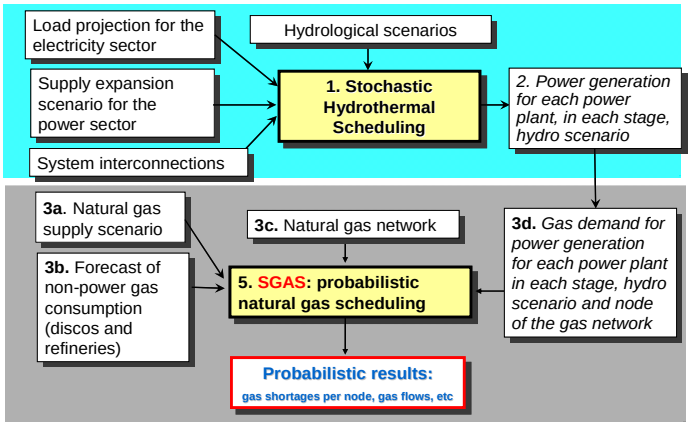

Figure 3 – data flow procedure

The lower shaded area shows the first step of the process: the use of a production-costing tool for hydrothermal scheduling based on Stochastic Dynamic Programming – it will be discussed next – that dispatches the power system for a given electric supply *x* demand configuration. The main driver of uncertainty is hydrology.

The result of interest is a set of power generation scenarios for each gas-fired power plant in each stage and simulated hydrological scenario for the study horizon. From these results and the consumption rates of each plant, a projection of the gas consumption for power generation is immediately obtained. The simulation is carried out for a set of hydrological scenarios, yielding a corresponding set of natural gas consumption scenarios. The shaded area in the upper part of Figure 3 represents the scheduling of the gas sector and verifies the "feasibility" of these scenarios under the gas sector point of view.

Each step will be discussed next.

4.1. Stochastic hydrothermal scheduling

Systems with considerable share of hydropower such as Brazil, Colombia, Norway and New Zealand, have been using hydrothermal scheduling tools for at least two decades. The objective of hydrothermal scheduling is to determine an operation strategy of a hydrothermal system that for each stage of the planning period produces generation targets for each plant (hydro releases and thermal production). This strategy should minimize the expected value of the operation cost along the period, composed of fuel cost and penalties for failure of load supply.

Hydro plants are dispatched based on their marginal water values, which are computed by a multi-stage stochastic optimization methodology, Stochastic Dual Dynamic Programming (SDDP) that approximates the cost-to-go functions by a set of linear inequalities, known as Benders cuts, avoiding the well know curse of dimensionality of traditional SDP models. The major advantage is the possibility to represent hydro plants individually. The SDDP approach is reviewed in great details in Annex A and it has been applied to the scheduling of large-scale power systems in more than thirty countries, including detailing modeling of system components and transmission networks [8].

However, as mentioned previously, the implementation of the SDDP algorithm in the majority of hydro-based countries as a dispatch model does not consider the gas supply-transportation constraints.

A simplified formulation of the one-stage problem solved in the SDDP recursion is shown next; further details can be found in [7-12] and in the Annex.

4.1.1. Objective function

The objective function is given by the minimization of thermal costs and rationing, plus a term that represents the cost-to-go function (also known as "future cost function").

$$\alpha_t\,(v_t,\, a_{t-1}) = \text{Min} \sum_{k=1}^{K} \sum_{j \in J} c_j \times g_{tk}(j) + c_\delta \times \delta + \alpha_{t+1}(v_{t+1}, a_t) \qquad (1.1)$$

where:

k	indexes load block in the stage
K	number of load blocks
j	indexes thermal plants
J	set of thermal plants
c_j	operating cost of plant j
$g_{tk}(j)$	Energy produced by thermal plant j (decision variable)
c_δ	generic representation of operating constraint violation cost
δ	violation amount (decision variable)
v_{t+1}	final storage vector in stage t (decision variable)
a_t	lateral inflow vector in stage t

The Future Cost Function is expressed as a scalar variable subject to linear inequalities (Benders cuts), which are determined according to the SDDP algorithm.

$$\alpha_{t+1}(v_{t+1}, a_t) = \quad \alpha$$

$$\text{s.t.} \quad \alpha \geq w_t(p) + \sum_{i \in I} \lambda_{tv}(i, p)\, v_{t+1}(i) + \sum_{i \in I} \lambda_{ta}(i, p)\, a_t(i) \quad p = 1, \ldots, P \qquad (1.2)$$

α	scalar variable that represents expected future operating cost
P	indexes segments of the piecewise future cost function
$w_t(p)$	constant term of p^{th} segment
$\lambda_{tv}(i, p)$	plant i's final storage coefficient in the p^{th} segment
$\lambda_{ta}(i, p)$	plant i's lateral inflow coefficient in the p^{th} segment
p	number of segments in the piecewise future cost function

4.1.2. Water balance equations

The *water balance* equation represents the coupling between successive stages: the reservoir storage v_{t+1} at stage $t+1$ is equal to the initial storage v_t minus outflow volumes (turbined variable u_t and spilled variable s_t) plus inflow volumes (lateral inflow a_t plus releases from immediately upstream plants belonging to set U), all in stage t, for all hydro plants in set K.

$$v_{t+1}(i) = v_t(i) + a_t(i) - \varepsilon(v_t(i)) - \sum_{k=1}^{K} [u_{tk}(i) + s_{tk}(i)] + \sum_{m \in M(i)} \sum_{k=1}^{K} [u_{tk}(m) + s_{tk}(m)]$$

$$\text{for } i \in I \qquad (1.3)$$

where:

i	indexes hydro plants
I	set of hydro plants
M(i)	set of upstream plants immediately upstream of plant i
$v_{t+1}(i)$	final storage of i in stage t (decision variable)
$v_t(i)$	initial storage of i in stage t
$a_t(i)$	lateral inflow to plant i
$\varepsilon(v_t(i))$	evaporated volume from reservoir i
$u_{tk}(i)$	turbined outflow volume of plant i along stage t in load block k (decision variable)
$s_{tk}(i)$	spilled outflow volume of plant i along stage t in load block k (decision variable)

4.1.3. Bounds on storage, turbined volumes and thermal generation variables

$$\underline{v}(i) \le v_t(i) \le \overline{v}(i) \qquad \text{for } i \in \text{I} \qquad (1.4)$$

$$u_{tk}(i) \le \overline{u}_t(i) \qquad \text{for } i \in \text{I};\ k = 1, \ldots, \text{K} \qquad (1.5)$$

$$\underline{g}_{tk}(j) \le g_{tk}(j) \le \overline{g}_{tk}(j) \qquad \text{for } j \in \text{J};\ \text{for } k = 1, \ldots, \text{K} \qquad (1.6)$$

4.1.4. Load balance equation

The *load supply* equation relates total thermal and hydro generation to system load d_t (MWh). The hydro generation for unit i is given by the product of its production coefficient $\rho(i)$ (MWh/m^3) and its turbined outflow $u_t(i)$, resulting in:

$$\sum_{i \in \text{I}} g_{hk}(i) + \sum_{j \in \text{J}} g_{tk}(j) = D_{tk} \qquad \text{for } k = 1, \ldots, \text{K} \qquad (1.7)$$

4.2. Probabilistic Gas Scheduling Model

A gas network consists of supply nodes, where the gas is injected into the system; demand nodes where gas flows out of the system due to thermal power or non-thermal use; and intermediate nodes. A pipeline is represented by an arc linking the nodes. When modeling gas pipelines for short-term scheduling studies, the gas flow through pipelines depends on the pressure difference between the entry and exit nodes; also, nonlinear expressions relate flow limits with the pressure in the pipeline [see e.g. 3,4,5,6]. For the purposes of the present study – long-term planning, with monthly steps – a linear network flow model was felt to be adequate. In this sense, the following constraints are modeled:

4.2.1. Gas Production and flow limits

Local production sources may be available at each node of the gas system. Operational constraints may impose daily minimum and maximum limits, represented by the following set of equations:

$$\underline{P}_t(n) \le P_t(n) \le \overline{P}_t(n) \qquad \text{for } n \in \text{N} \qquad (2.1)$$

where $P_t(n)$ is the gas production at node n (decision variable), stage t and the pair $\{\underline{P}_t(n), \overline{P}(n)\}$ is respectively the minimum and maximum production limits at node n, stage t represents the production curve of the gas field. Finally N is the set of gas nodes.

The nodes of the gas system are interconnected by pipelines. Each pipeline can be characterized by its maximum and minimum flow limits under equilibrium (steady state) conditions, originating the following constraints:

$$\underline{f}_t(n,l) \le f_t(n,l) \le \overline{f}_t(n,l) \qquad \text{for } n,l \in \text{N} \qquad (2.2)$$

where $f_t(n,l)$ is natural gas flow in the pipeline (decision variable) that connects nodes n and l and the pair $\{\underline{f}_t(n,l), \overline{f}_t(n,l)\}$ is respectively the minimum and maximum flow limit between nodes n and l.

4.2.2. Gas Balance equations

At each stage, the sum of the demands at each node must be equal to the sum of the supply – either locally produced or imported through the pipelines – and of the deficit – in case there is not enough natural gas to completely fulfill the demand. For each node of the gas system, we have:

$$P_t(n) + \sum_{l \in \Omega(n)} [1 - w_t(n,l)]\, f_t(l,n) - \sum_{l \in \Omega(n)} f_t(n,l) + \sum_{k \in D(n)} \delta_t(k) + \sum_{j \in T(n)} \delta_t'(j) = \sum_{k \in D(n)} d_t(k) + \sum_{j \in T(n)} \phi_t(j)\, g_t^*(j)$$

$$\text{for } n \in N \qquad (2.3)$$

where $\Omega(n)$ is the set of nodes of the gas system connected to node n, $T(n)$ is the set of thermal plants associated to node n of the gas system and $D(n)$ is the set of non-thermoelectric demands at node n of the gas system (distribution companies, refineries, and others). The parameters are: $w_t(n,l)$ for the loss factor of the pipeline connecting nodes n and l and $\phi_t(j)$ for the gas consumption conversion factor for thermal plant j and $d_t(k)$ is the non-electric natural gas demand k. The generation of the gas-fired plant j, $g_t^*(j)$ is also known in this context, as it is obtained from the hydro scheduling simulation.

The decision variables of the problem are: (i) scheduling of gas supply sources; (ii) scheduling of gas flows in the pipelines and (iii) deficits of natural gas for non-electrical demand k, $\delta_t(k)$ and the deficit of natural gas for thermal power plant j, $\delta_t'(j)$. They appear in the objective function associated with costs c_k and c_j' - the deficit cost for the natural gas non-electrical demand k and the electrical demand j, respectively.

4.2.3. Objective Function

The objective function is to minimize the natural gas rationings costs, thus:

$$Min \sum_k c_k \delta_t(k) + \sum_j c_j' \delta_t'(j) \qquad (2.4)$$

4.3. Case Study

The probabilistic evaluation scheme will be illustrated with basis on the (publicly available) power system configuration of the Brazilian Monthly Operations Plan ("PMO") for December 2005-December 2009. As shown in Figure 3, the stochastic operational policy for 2005/2009 was calculated (with five additional years as a buffer to prevent depletion at the end of the period) using the SDDP hydrothermal dispatch algorithm previously described. Monthly steps were used, with three demand blocks in each step. Once the hydrothermal operational policy was calculated, the system operation was simulated for a set of hydrological scenarios, resulting in energy production schedules for each gas-fired power plant, for each month and for each hydrological scenario.

Next, these energy production schedules were transformed into gas consumption schedules, though the use of efficiency factors for each power plant. Finally, these gas schedules were added to the "non-power" gas consumption forecasts at the appropriate consumption nodes.

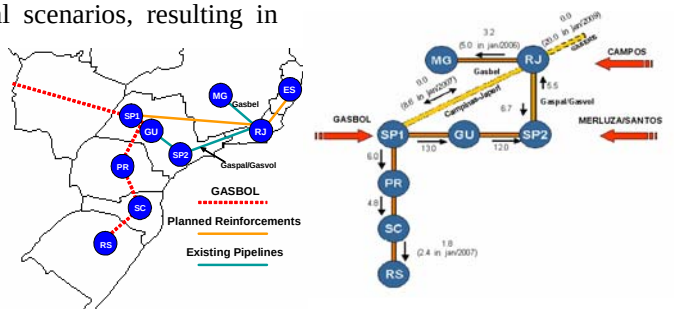

Figure 4 – South/Southeast gas network

Table 1 shows the gas supply projections, including production increase in local fields and imports. Figure 4 shows the pipeline network for the South-Southeast region. A similar procedure was applied for the Northeast network (remember that the gas networks are not integrated yet).

Finally, the "non-power" gas consumption was estimated for each sector (industrial, automotive, commercial, residential and co-generation), in addition to Petrobras (Brazil's oil and gas company) internal consumption in refineries and fertilizer plants. Figure 5 compares total supply and demand for the years of study. We see that the gas consumption from thermal plants is crucial for the demand x supply balance: if the thermal plants are not dispatched at all along the year (zero consumption of power-related gas), supply exceeds demand; at the other extreme, if the thermal plants are 100% dispatched along the year (base-loaded), supply cannot match demand. Given that the thermal plant dispatch depends, as seen previously, on hydrological conditions and on the overall supply s demand balance of the electricity sector, the question is then to assess the likelihood and severity of the gas supply shortfalls.

Table I – Gas supply projection available to market

(MMm3/day)		*2006*	*2007*	*2008*	*2009*
South/Southeast					
	Campos	14.4	14.9	15.5	15.0
	Merluz a + Lagosta	1.2	1.9	1.9	1.9
	Gasbol	30.0	30.0	30.0	30.0
	TSB	0.0	0.0	0.0	0.0
	Santos	0.0	0.0	12.0	12.0
Total		45.6	46.8	59.4	58.9
Espírito Santo					
Total		4.4	6.6	10.0	10.0
Northeast					
Total		14.2	15.4	14.4	13.4
Brazil					
Total		64.2	68.8	83.8	82.3

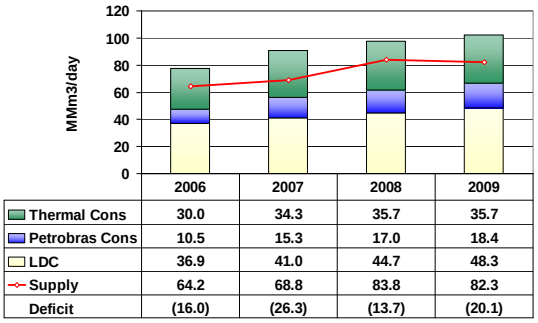

Figure 5 – Gas supply x demand balance

Figure 6 shows the frequency of gas supply shortfalls in volumes higher than 5% of the gas-to-power demand. Figure 7 shows the cumulative duration curve of the gas volumes shortfall, expressed in average MW (in other words, assuming that the supply of "non power" demand has priority over the supply of power-related consumption). We see in Figure 6 that in 2007, 19% of the scenarios had shortfalls; in turn, Figure 7 shows that the severity of the shortfalls in concentrated in fewer scenarios, which is consistent with the skewed probability distribution of droughts ("wet" scenarios are more likely than dry scenarios).

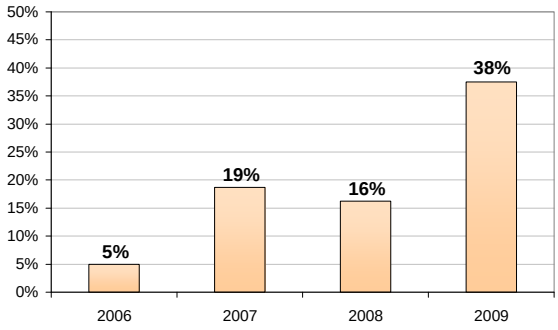

Figure 6 – Gas deficit probability

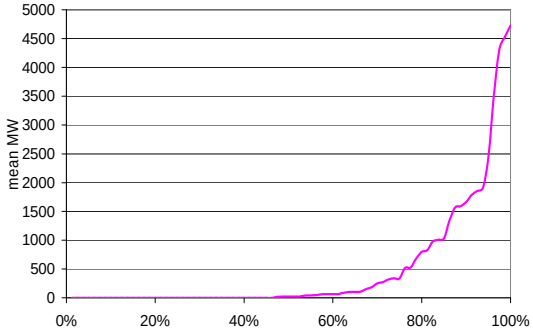

Figure 7 – Gas deficit distribution in 2007

5. Integrated electricity-gas modeling in hydro scheduling models

The previous study showed that the probability of dispatch failures of gas-fired plants due to fuel supply problems could be significant. Given that the hydrothermal dispatch model did not "know" about this possibility when calculating the water value of the hydroelectric plants, this means that the hydrothermal dispatch is not fully optimized: the system reservoirs will be depleted faster than expected, thus increasing the risks of energy deficits or of dispatching more expensive thermal plants such as fuel oil and diesel. One clear possibility for improving this situation is to incorporate the gas supply equations and constraints into the stochastic hydrothermal model, as described next.

5.1.1. Gas pipeline equations

The set of equations (2.1)-(2.3) is added to the one-stage presented problem formulation above. The only change lies in equation (2.3): thermal generation values $g_t^*(j)$ were known values in problem (2.1)-(2.4) and are decision variables $g_t(j)$ here. The modified equation becomes:

$$P_t(n) + \sum_{l\in\Omega(n)} [1-w_t(n,l)]\, f_t(l,n) - \sum_{l\in\Omega(n)} f_t(n,l) + \sum_{k\in D(n)} \delta_t(k) + \sum_{j\in T(n)} \delta_t'(j) - \sum_{j\in T(n)} \phi_t(j)\, g_t(j) = \sum_{k\in D(n)} d_t(k)$$

$$\text{for } n \in N \qquad (3.1)$$

5.2. Case study

The integrated electricity-gas hydrothermal scheduling was applied for the same electricity-gas configuration and data of the previous analysis. Also as in the previous study, we gave more priority for the "non power" gas supply than for gas-fired generation, in case of fuel shortages.

Figure 8 shows the yearly short-run marginal cost (SRMC) of electricity (averaged over all months, load levels and hydrological scenarios) of the Southeast system for two situations: unrestricted gas supply and supply constraints. We see that the fuel supply constraints had an important effect on electricity costs. Figure 9 shows the distribution of yearly SRMC over the hydrological scenarios, again for the fuel-constrained and unconstrained cases. We see that fuel constraints did not affect electricity prices in most hydrological scenarios, which are "wet" and do not require thermal generation. However, they had a large impact on the remaining dry scenarios.

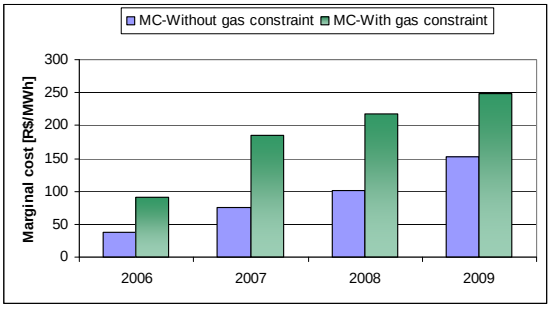

Figure 8 - Annual SRMC – Southeast region

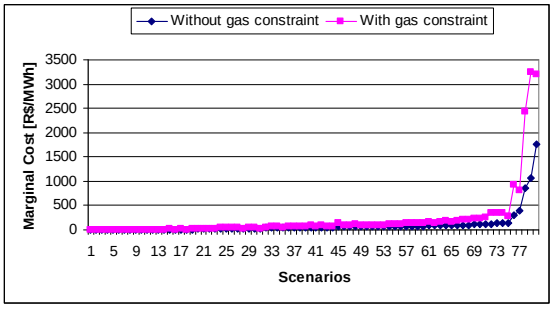

Figure 9 - Distribution of the Southeast System marginal cost in 2008

The impact of the natural gas constraints to the gas-fired thermal generation is shown in Figures 10 and 11. Figure 10 compares the maximum and mean total generation for both cases - with and without the constraints. The maximum generation of the case with no constraints is nearly twice as much as the one with the constraints. The mean generation, in turn, is more similar in both cases. The likely reason for this is that when constraints are included in the policy calculation of the stochastic dual dynamic programming algorithm, there is a tendency for the occurrence of preventive thermal generation to compensate for a smaller firm power availability caused by the gas constraints. The end effect is not a big change in the *mean* generation, but rather, in the tails of the distribution. In other words, the consideration of the gas constraints will be result in less generation for the critical scenarios, but a higher generation for the moderate scenarios. This effect can be clearly seen in Figure 11. Notice that the case with the generation constraints has much less amplitude then the other (values are sorted following the results of the simulation without gas constraints).

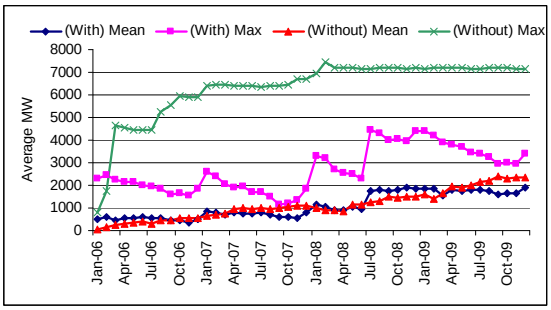

Figure 10 – Mean and maximum gas-fired generation

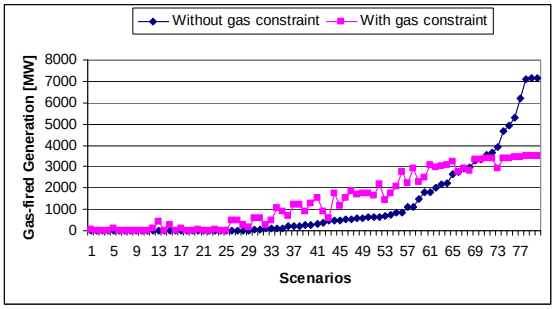

Figure 11 - Distribution of the gas-fired thermal power generation in 2008

The impact of gas supply constraints on electricity prices could be alleviated by other measures, which can also be evaluated by the integrated gas-electricity scheduling model. One possibility is to transform the gas-fired plants into bi-fuel plants (the other fuel being diesel oil). Another possibility, is to negotiate interruptible (flexible) gas contracts with industry, which would switch to an alternative

fuel or even decrease production in case the gas-fired plants were dispatched. These alternatives bring more flexibility to the electricity-gas market and should be evaluated in a future work.

6. Conclusions

The vigorous growth of the natural gas market in hydro-dominated countries poses special challenges for planning and operations scheduling of both the electricity and gas sectors due to the substantial oscillation in power-related gas consumption when hydrological conditions vary from "wet" to "dry". In this paper, we examined two alternatives for coordinating these sectors. In the first one, power dispatch assumes that there are no fuel constraints and produces a (stochastic) gas consumption schedule which is added to the "non power" gas consumption forecasts, all to be managed by the gas dispatch. In the second alternative, power and gas are dispatched jointly. It is shown that both alternatives can be modeled by stochastic optimization techniques, and their application is illustrated in case studies based on realist data from the Brazilian power system. It should be noted that this type of modeling and analysis, introduced by these authors, are being the basis of the studies and evaluations currently carried out by Brazilian authorities on this subject in the country.

7. BIBLIOGRAPHY

[1] Barroso, L.A.; Flach, B.; Kelman, R.; Bezerra, B.; Binato, S.; Bressane, J.M.; Pereira, M.V.; "Integrated gas-electricity adequacy planning in Brazil: technical and economical aspects" Proceedings of the IEEE PES General Meeting, San Francisco, 2005.

[2] IEA – South American Gas – Daring to tap the bounty, IEA Press, 2003

[3] R.R. Mercado, "Natural Gas Pipeline Optimization", Handbook of Applied Optimization, Edited by P. M. Pardalos and M. G. C. Resende, Oxford university Press, 2002

[4] D. Wolf and Y. Smeers. "The gas transmission problem solved by an extension of the simplex algorithm", Management Science, vol 46, no. 11, pp. 1454-1465, Novembro, 2000

[5] J. Munoz, N.J. Redondo, J.P. Ruiz, "Natural gas network modeling for power systems reliability studies", IEEE PES-Summer Meeting, Chicago, 2002

[6] O.D. Mello, T. Ohishi, "Natural Gas Transmission for Thermoelectric Generation Problem", IX Simpósio de Especialistas em Planejamento da Operação e Expansão Elétrica, Maio, 2004

[7] M.V.Pereira, N. Campodónico, and R. Kelman, "Long-term hydro scheduling based on stochastic models", Proceedings of EPSOM Conference, Zurich, 1998 – Available at http://www.psr-inc.com

[8] S. Granville, G. C. Oliveira, L. M. Thomé, N. Campodónico, M. L. Latorre, M. Pereira, L. A. Barroso, "Stochastic Optimization of Transmission Constrained and Large Scale Hydrothermal Systems in a Competitive Framework," Proceedings of the IEEE General Meeting, Toronto, 2003.

[9] M.V.F. Pereira and L.M.V.G. Pinto, "Operation Planning of Large-Scale Hydrothermal Systems", Proceedings of the 8th PSCC, Helsinki, Finland, 1984.

[10] M.V.F. Pereira and L.M.V.G. Pinto, "Stochastic Optimization of Multireservoir Hydroelectric System – a Decomposition Approach", Water Resource Research, Vol 21 No 6, 1985.

[11] B.G. Gorenstin, N.M. Campodónico, J.P. Costa, M.V.F. Pereira, "Stochastic Optimization of a Hydrothermal System Including Network Constraints", IEEE Transactions on PAS, Vol. 7, No. 2, May 1992.

[12] Application of Stochastic Dual DP and Extensions to Hydrothermal Scheduling – PSR TR 012/99 – available at http://www.psr-inc.com

[13] ISO NEW ENGLAND INTERNAL REPORT on natural gas shortage, available at: http://www.iso-ne.com/special_studies/Interim_Report_on_January_14_-_16_2004_Cold_Snap/

[14] Read, E. and George, J., "Dual dynamic programming for linear production/inventory systems", Computers and Mathematics with Applications", 19(11), 29-42, 1990.

8. BIOGRAPHIES

Bernardo Bezerra has a BSc in Electrical and Industrial Engineering and an MSc degree in Optimization, both from PUC-Rio. He joined PSR in 2004 and has been working in several projects

related to demand forecasting, stochastic optimization models, synthetic streamflow generation and integrated electricity-gas planning

Luiz Augusto Barroso has a BSc in Mathematics and an MSc and PhD in optimization from COPPE/UFRJ. He joined PSR in 1999, where he has been working in project economics evaluation, system planning studies, integration between electricity and gas and market power analysis in energy markets. He has been a speaker on power system planning and operations issues in Latin America, Europe and US/Canada.

Rafael Kelman has a B.Sc degree in Water Resources Engineering, a MSc degree in Operations Research and is finalizing a PhD in OR. He joined PSR in 1997, where he has worked in several projects related to economic evaluation of hydro and thermal projects, strategic bidding, water pricing and allocation and transmission pricing. He has been working in the development of a short term scheduling model with unit commitment. Mr. Kelman has been an instructor of several PSR courses in Europe, South America and the US. His research interests include water resources, stochastic optimization, planning under uncertainty and finance.

Bruno Flach has a BSc in Electrical and Industrial Engineering and is currently working towards a MSc degree in Optimization, both from PUC-Rio. He joined PSR in 2002 and has been working in various projects related to software development and technical support, demand forecasting and optimization models. Mr. Flach's research interests are now focused on stochastic optimization and strategic bidding.

Maria de Luján Latorre has a BSc degree in Mathematics from UNR, Argentina and a PhD degree in Systems Engineering (optimization) from COPPE/UFRJ. She joined PSR in 2001, where she is working on the development and study in Power Systems Optimization area. Previously, she worked at CEPEL (the Brazilian electrical research center), where she developed computational tools for optimal power flow.

Nora Campodónico has a BSc degree in Statistics from the Catholic University of Lima and a DSc degree in Systems Engineering (optimization) from COPPE/UFRJ. She joined PSR in 1992, where she coordinates the development of software products in the areas of stochastic hydrothermal scheduling, power system planning under uncertainty and competition, reliability evaluation and optimal pricing.

Mario Veiga Pereira has a BSc degree in EE from PUC/Rio and PhD degree in Optimization from COPPE/UFRJ. He is the president of PSR and he is currently engaged in regulatory studies and the development of new methodologies and tools for risk management in competitive markets. Previously he was a project manager at EPRI's PSPO program and research coordinator at Cepel, where he developed methodologies and software for expansion planning, reliability evaluation and hydrothermal scheduling. He was one of the recipients of the Franz Edelman Award for Management Science Achievement, granted by ORSA/TIMS for his work on stochastic optimization applied to hydro scheduling.

ANNEX A: HYDROSCHEDULING AND THE SDDP ALGORITHM

The objective of hydrothermal scheduling is to determine the sequence of hydro releases, which minimizes the expected thermal operation cost (given by fuel cost plus penalties for rationing) along the planning horizon. Nevertheless, the availability of this hydro energy is limited by reservoir storage capacity. Therefore, there is a relationship between the operative decision in a given stage and the future consequences of this decision. For example, if the stored hydroelectric energy is used today, and a drought occurs, it may be necessary to use expensive thermal generation in the future, or even interrupt the energy supply. If, on the other hand, reservoir levels are kept high through a more intensive use of thermal generation today, and high inflows occur in the future, reservoirs may spill and waste energy, resulting in increased operation costs. Figure A.1 illustrates this decision tree.

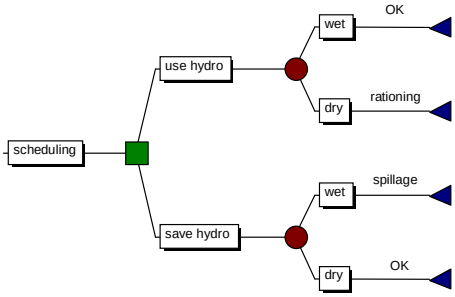

Figure A.1 - Decision Process for Hydrothermal Systems

In contrast with thermal systems, whose long-term operation is decoupled in time, hydro system operation is *coupled* in time, so a decision today affects operating costs in the future. Also, since future inflows are unknown and difficult to forecast, the scheduling of hydrothermal systems is essentially stochastic.

The scheduling problem is decomposed into several one-stage subproblems, where the objective is to minimize the sum of *immediate* and *future* operating costs, where the tradeoff between *immediate* and *future* operating costs is illustrated in Figure A.2.

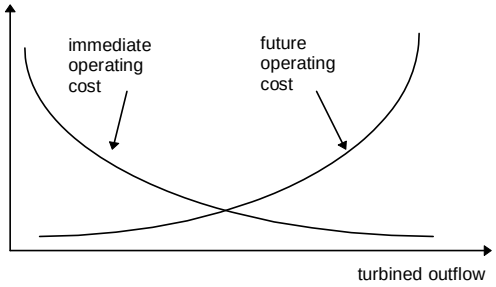

Figure A.2 - Immediate and future operation costs as a function of final storage

The immediate cost function (ICF) is related to thermal generation costs in the present stage. The more the stored water is used for energy production, the cheaper the ICF will be today, since less thermal generation is needed to meet the load. However, using more water today leaves less storage for future use. So, in terms of the final storage, the ICF increases for higher final storage values. In turn, the future cost function (FCF) is associated with the *expected* thermal generation expenses from the next stage to the end of the study period. We see that the FCF decreases with final storage, as more water becomes available for future use.

Conceptually, the FCF can be obtained by simulating the system operation in the future for different starting values of initial storage and calculating the operation costs. If the capacity is relatively small, as in the Spanish or Norwegian system, the impact of a decision is diluted in several months. If the

capacity is substantial, as in Brazil, the simulation horizon may reach five years. The simulation must take into account the *variability* of inflows to reservoirs, which fluctuate seasonally, regionally and from year to year. Inflow forecasts are generally inaccurate, in particular when it comes from rainfall, not snowmelt. Therefore, inflows are usually modeled as a multivariate stochastic process which preserves relevant serial and spatial dependencies observed in the past. As a consequence, FCF calculation has to be carried out on a *probabilistic* basis, using a large number of hydrological scenarios.

The optimal use of stored water corresponds to the point that minimizes the sum of immediate and future costs. As shown in Figure A.3, this is also where the derivatives of ICF and FCF (in absolute value) with respect to storage are equal. These derivatives are known as water *values*. The optimal hydro dispatch is at the point that equalizes immediate and future water values.

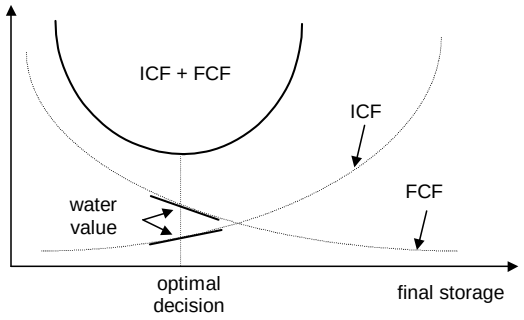

Figure A.3 - Optimal hydro scheduling

A.1 Formulation of One-Stage Hydrothermal Dispatch

The immediate cost is given by the thermal operating costs in stage *t*, $\sum_{j \in J} c(j)g_t(j)$, where J denotes the set of thermal plants, c is the vector of thermal unit operating costs and variable g_t (MWh) is the vector of thermal generations in stage *t*. In turn, the future cost is represented by the function $\alpha_{t+1}(v_{t+1})$, where variable v_{t+1} is the vector of reservoir levels in stage *t+1*. Let us consider independent inflow scenarios. Given the initial storage vector v_t, the objective of the one-stage hydroscheduling problem is to minimize the sum of immediate and future discounted operating costs (β is the discount factor):

$$(1)\quad z_t(v_t) = \min \sum_{j \in J} c(j)g_t(j) + \beta\, \alpha_{t+1}(v_{t+1})$$

Plant operation is modeled through the following constraints. The *water balance* equation (shown in Figure A-4) represents the coupling between successive stages: the reservoir storage v_{t+1} at stage *t+1* is equal to the initial storage v_t minus outflow volumes (turbined variable u_t and spilled variable s_t) plus inflow volumes (lateral inflow a_t plus releases from immediately upstream plants belonging to set *U)*, all in stage *t*, for all hydro plants in set *I:*

$$(2)\quad v_{t+1}(i) = v_t(i) - u_t(i) - s_t(i) + a_t(i) + \sum_{m \in U(i)} [u_t(m) + s_t(m)],\ i \in I$$

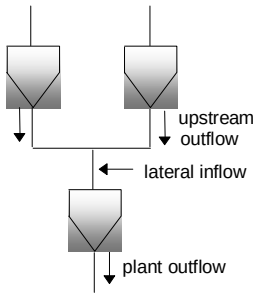

Figure A.4 - Reservoir water balance

The *load supply* equation relates total thermal and hydro generation to system load d_t (MWh). The hydro generation for unit i is given by the product of its production coefficient $\rho(i)$ (MWh/m^3) and its turbined outflow $u_t(i)$, resulting in

$$(3)\quad \sum_{i \in I} \rho(i) u_t(i) + \sum_{j \in J} g_t(j) = d_t$$

Finally, there are bounds on thermal generation (g_{max}), maximum storage (v_{max}) and turbine capacity (u_{max}) for each hydro plant:

$$(4)\quad g_t(j) \leq g_{max},\ j \in J$$

$$(5)\quad v_{t+1}(i) \leq v_{max}(i),\ i \in I$$

$$(6)\quad u_t(i) \leq u_{max}(i),\ i \in I$$

For simplicity, network constraints are not represented in the above formulation. These constraints are not coupled in time, and are expressed as linearized power flow equations with transmission limits.

A.1.1 Calculation of Future Cost Function

The future cost function calculation is naturally the key aspect of the state-space scheme. In theory, $\alpha_{t+1}(v_{t+1})$ could be calculated by *simulating* system operation in the future for different starting values of initial storage and calculating the operating costs, as illustrated in Figure A.5.

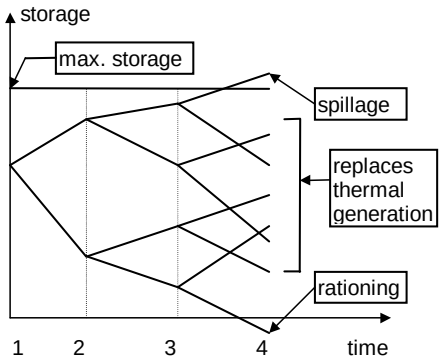

Figure A.5 - "Brute Force" FCF Calculation

However, this "brute force" approach has the same computational drawbacks as the explicit stochastic formulation. Therefore, the future cost function in each stage is calculated through a more efficient *stochastic dynamic programming* (SDP) recursion: reservoir levels are discretized, and starting from the last stage *T*, problem (1-6) is solved assuming the first storage level for each reservoir. Since we are at the last stage, the FCF is zero. Because of inflow uncertainty, the hydro scheduling problem is successively solved for *N* different inflow scenarios and the expected operation cost is calculated as the mean of the costs over the *N* scenarios. For each remaining storage states in stage *T*, repeat the calculation of expected operation costs and interpolate in order to produce the FCF $\alpha_T(v_T)$ for stage *T-1*. This process is then repeated for all states is stages *T-1*, *T-2* etc. Note that the objective in those stages is to minimize immediate operation plus expected future cost, given by previously calculated FCF. The final result of the SDP scheme outlined above is the set of future cost functions $\alpha_{t+1}(v_{t+1})$ for each stage *t*.

The procedure can be depicted as follows:

initialize the end-of-horizon future cost function $\alpha_{T+1}(v_T) \leftarrow 0$

for t = T, T-1, ..., 1

for each storage value $v_t = v_t^1, ..., v_t^m, ..., v_t^M$

for each inflow scenario $a_t = a_t^1, ..., a_t^k, ..., a_t^K$

solve the one-stage problem (4.1) for initial storage v_t^m and inflow a_t^k:

$$\alpha_t^k(v_t^m) = \quad \text{Min} \quad c_t(u_t) + \alpha_{t+1}(v_{t+1})$$

subject to (4.2)

$$v_{t+1} = v_t^m - u_t - s_t + a_t^k$$

$$v_{t+1} \le \overline{v}$$

$$u_t \le \overline{u}$$

next

calculate the expected operation cost over all inflow scenarios:

$$\alpha_t(v_t^m) = \sum_{k=1}^{K} p_k \times \alpha_t^k(v_t^m)$$

next

create a complete future cost function $\alpha_t(v_t)$ for the previous stage by interpolation on the discrete values $\{\alpha_t(v_t^m), m = 1, ..., M\}$

next

However, due to the discretization, the SDP computational effort increase exponentially with the number of reservoirs, the well-known "curse of dimensionality" of DP. Therefore, it is not practical for systems with many reservoirs.

For this reason, it has become necessary to develop computationally feasible state-space schemes. The traditional approach, still adopted in many countries, has been to reduce system dimensionality by the aggregating system reservoirs into one reservoir that represents the energy production capability of the cascade. This scheme is in some cases coupled with the use of partial dynamic programming schemes (typically, calculation of separate future cost functions for each basin).

More recently, an approach based on the analytical representation of the future cost function, known as stochastic *dual* dynamic programming (SDDP) has been applied in several countries in South and Central America, plus USA, New Zealand, Spain and Norway[2]. The SDDP scheme does not require discretization of the state space and, as a consequence, alleviates the computational requirements of the stochastic DP recursion. It will be described next.

A.2.2 The Dual Dynamic Programming Scheme

The stochastic dual DP scheme (DDP) proposed independently by [10] and [14] is based on the observation that the FCF can be represented as a piecewise linear function, so there is no need to create an interpolated table. Furthermore, the slope of the FCF around a given point can be analytically obtained from the one-stage dispatch problem (1-6).

The last-stage dispatch problem is shown below (note that the FCF in this stage is zero):

(7) $z_T = min \sum_{j \in J} c(j) g_T(j)$

(8) $v_{T+1}(i) = v_T(i) - u_T(i) - s_T(i) + a_T(i) + \sum_{m \in U(i)} [u_T(m) + s_T(m)], i \in I$

(9) $\sum_{i \in I} \rho(i) u_T(i) + \sum_{j \in J} g_T(j) = d_T$

[2] A related scheme, called constructive dynamic programming, has been applied to the Australian system .

(10) $g_T(j) \leq g_{max}, j \in J$

(11) $v_{T+1}(i) \leq v_{max}(i), i \in I$

(12) $u_T(i) \leq u_{max}(i), i \in I$

The Lagrange multiplier vector π_h associated to the water balance equation (8), also known as the *water value*, represents the derivative of z_T with respect to a variation in the initial storage v_T, and corresponds to the slope of FCF for stage *T-1*. Figure A.6 shows the calculation of the operation cost and FCF slopes for each state in stage *T*. It can be seen that the FCF for stage *T-1* corresponds to the *piecewise* cost surface produced by taking the linear segment with the highest cost value in each state (the convex hull).

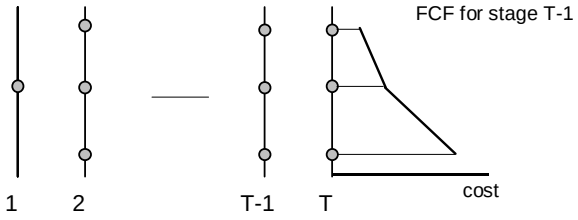

Figure A.6 - Calculation of Piecewise FCF for stage T-1

The dispatch problem for stage *T-1* is now

(13) $z_{T-1}(v_{T-1}) = min \sum_{j \in J} c(j) g_T(j) + \beta \alpha_T$

(14) $v_T(i) = v_{T-1}(i) - u_{T-1}(i) - s_{T-1}(i) + a_{T-1}(i) + \sum_{m \in U(i)} [u_{T-1}(m) + s_{T-1}(m)], i \in I$

(15) $\sum_{i \in I} \rho(i) u_{T-1}(i) + \sum_{j \in J} g_{T-1}(j) = d_{T-1}$

(16) $g_{T-1}(j) \leq g_{max}, j \in J$

(17) $u_{T-1}(i) \leq u_{max}(i), i \in I$

(18) $\alpha_T \geq \varphi_T^n v_T + \delta_T^n, n=1,\ldots,N$

The future cost function is represented by the scalar variable α_T and the *N* linear constraints $\{\alpha_T \geq \varphi_T^n v_T + \delta_T^n\}_{n=1,N}$ where *N* is the number of linear segments. A shown in Figure A.7, these inequalities represent the piecewise characteristic of this function.

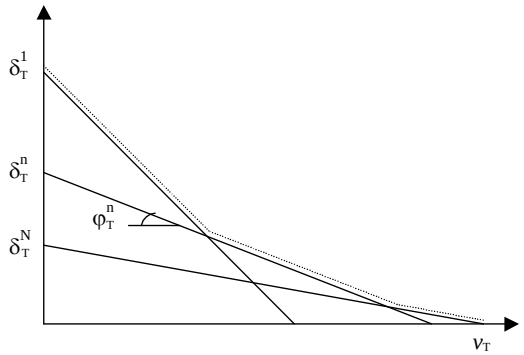

Figure A.7 - Piecewise linear FCF for stage T

Therefore in general, for each stage *t*, the FCF is represented by the scalar variable α_t and *N* linear constraints.

A.2.1.1 Backward Recursion and Lower Bound Calculation

The recursive calculation of the piecewise linear FCF is very similar to the standard SDP scheme. In order to take into account that future inflows are unknown consider *K* inflow scenarios. The backward recursion scheme is shown below:

Set N equal to M, the number of initial storage values;

initialize the FCF for stage T as zero: δ^n_{T+1} *and* φ^n_{T+1} *are null, for n=1,…,N;*

for t=T,T-1,…,1

for each storage value v_t^m*, m=1,…,M*

for each inflow scenario a_t^k*,k=1,…,K*

solve the one-stage scheduling problem for initial storage v_t^m *and inflow* a_t^k *:*

(19) $z_t^k(v_t^m) = min \sum_{j \in J} c(j)g_t(j) + \beta\, \alpha_{t+1}$

(20) $v_{t+1}(i) = v_t^m(i) - u_t(i) - s_t(i) + a_t^k(i) + \sum_{m \in U(i)} [u_t(m) + s_t(m)],\ i \in I$

(21) $\sum_{i \in I} \rho(i)u_t(i) + \sum_{j \in J} g_t(j) = d_t$

(22) $g_t(j) \le g_{max},\ j \in J$

(23) $u_t(i) \le u_{max}(i),\ i \in I$

(24) $\alpha_{t+1} \ge \varphi^n_{t+1}\, v_{t+1} + \delta^n_{t+1},\ n=1,\ldots,N$

end;

calculate the volume coefficients and constant term for the m^{th} *linear segment of FCF in the previous stage by taking averages over all scenarios (scenario k at stage t has conditional probabilility* p_{kt}*):*

(25) $\varphi_t^m = \sum_k p_{kt}\, \pi_{ht}^{\ k}$

(26) $\delta_t^m = \sum_k p_{kt}\, \alpha_t^k(v_t^m) - \varphi_t^m\, v_t^m$

end;

end.

At first sight, there are no substantial differences between the Dual DP procedure in and the traditional DP scheme. Note, however, that the traditional scheme had to create a new future cost function table in each stage by *interpolation* of the discrete values $\{\alpha_t(v_t^m)\}$. As a consequence, the required number of points in the table for a system of I hydro plants is at least equal to the 2^I combinations of extreme points (full/empty). In the Dual DP scheme, the piecewise linear segments can be used to *extrapolate* the future cost function values, i.e. it not necessary to use all combinations of points to obtain a complete (although approximate) future cost function. Moreover, if a smaller number of initial storage values is used, a smaller number of linear segments will be generated. As seen in Figure A-7, the resulting future cost function, which is based on the maximum value over all segments, will then be a *lower bound* to the "true" function.

As a consequence, the future cost function for the first stage is a lower bound $\underline{z}$ to the optimal solution of the hydrothermal scheduling problem:

(27) $z^L = z_1(v_1)$

A.2.1.2Forward Simulation and Upper Bound Calculation

If we use the FCF produced by the backward recursion scheme, an upper bound to the optimal solution of the hydrothermal scheduling problem can be obtained by Monte Carlo simulation of system operation ([14] uses a complete representation of the piecewise linear function; his approach was limited to two reservoirs). This is due to the fact that the only FCF that can result in the optimal operation cost is the optimal function itself; all others, by definition, will have higher operation costs. The simulation scheme is shown below.

Define inflow scenarios a_t^m*, m=1,…,M for all stages t=1,…,T;*

for each inflow scenario a_t^m, m=1,…,M

initialize storage value for stage 1 as $v_t^m = v_1$;

for t=1,…,T

solve the one-stage scheduling problem (19-24) ;

calculate the total operating cost z^m for scenario m as the sum of all immediate thermal costs along the study period;

end;

end.

An upper bound for the expected operation cost is estimated as the mean total cost over all scenarios:

$$(28)\ z^U = M^{-1} \sum_{m=1,M} z^m$$

This estimator is unbiased, converging to the population value. Due to the sampling variation, there is an uncertainty around the "true" expected value. A 95% confidence interval $[z^U-1.96\sigma, z^U+1.96\sigma]$ can be derived by estimating the variance of the estimator as

$$(29)\ \sigma^2 = M^{-1} \sum_{m=1,M} (z^m - z^U)^2$$

A.2.1.3..Optimality Check and New Iteration

Optimality is achieved when the lower bound z^L is within the confidence interval of the upper bound. Note that because of sampling variation, the lower bound may exceed the upper bound mean estimate z^U.

If the lower bound is outside the confidence interval, the backward recursion step described previously is repeated with an additional set of storage values. These values are produced by the forward simulation step. Note that all linear constraints produced along the iterative process are retained, since the piecewise FCF is given by the convex hull. Therefore, the representation of the FCF is gradually improved along the process until convergence is achieved.